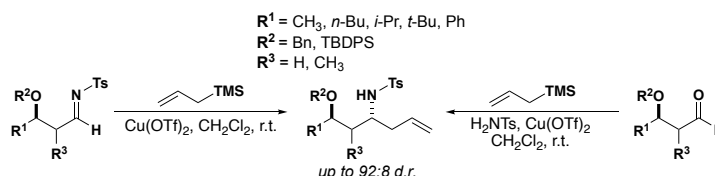


# 1,3-Asymmetric Induction in Diastereoselective Allylations of Chiral *N*-Tosyl Imines

Anna Lo, David A. Gutierrez, Garrett Toth-Williams, James C. Fettingner and Jared T. Shaw\*

Department of Chemistry, University of California, Davis, Davis California, 95616, United States

Supporting Information Placeholder



**ABSTRACT:** Lewis-acid mediated allylations of  $\beta$ -alkoxy *N*-tosyl imines lead to 3-alkoxy homoallylic *N*-tosyl amines with *anti* diastereoselectivity. Diastereoselectivity and yields of reactions are comparable between two methods of Hosomi-Sakurai allylations. Observed selectivity trends and computational evidence suggest that 1,3 asymmetric induction occurs through the formation of a six-membered ring chelate which adopts a half-chair-like conformation. The product ratios of allylations to  $\beta$ -alkoxy *N*-tosyl imines are dependent on conformation preferences of the chelate and stereoelectronic interactions in the transition-state structures. Debenzylation and detosylation of these allylation products result in *anti* 1,3-amino alcohols, a privileged motif in synthetic and natural bioactive compounds.

The use of resident stereogenic centers to control the outcome of diastereoselective reactions is a powerful strategy for the construction of complex organic molecules. Although the influence of both  $\alpha$  and  $\beta$  stereogenic centers on the addition of nucleophiles to aldehydes has been thoroughly studied, analogous studies of  $\alpha$ - and  $\beta$ -substituted electron-deficient imines are sparse. We recently disclosed the first comprehensive study of  $\alpha$ -alkoxy imines and demonstrated high levels of either syn or anti diastereoselectivity based on the nature of the nucleophilic alkene employed.<sup>1</sup> That study also demonstrated that the typically mono-coordinate Lewis acid  $\text{BF}_3 \cdot \text{OEt}_2$  can form a highly reactive chelate by disproportionation to  $\text{BF}_2^+/\text{BF}_4^-$ . Based on these observations, we sought to explore the factors influencing acyclic stereocontrol in  $\beta$ -alkoxy imines, allowing access to chiral 1,3 amino alcohols, a common motif in biologically active synthetic targets (Figure 1).<sup>2,3</sup>

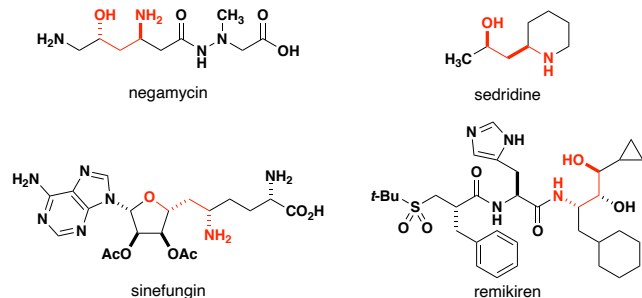


**Figure 1.** Examples of biologically active anti-1,3 amino alcohols.

Previously reported examples of Lewis acid mediated nucleophilic additions to  $\beta$ -alkoxy aldehydes show how 1,3 asymmetric induction in  $\beta$ -alkoxy aldimines can result in highly selective reaction outcomes. Chelateable Lewis acids used in nucleophilic additions to  $\beta$ -alkoxy aldehydes lead to *anti-2* in high diastereomeric ratios. Reetz<sup>4</sup>, Keck<sup>5,6</sup> and Heathcock<sup>7</sup> rationalized this observed *anti* selectivity through the preferential approach of a nucleophile on the less hindered side of a six-membered chelate (Figure 2, A). Evans later reported comparable *anti* selectivity in Mukaiyama aldol additions to  $\beta$ -alkoxy aldehydes with  $\text{BF}_3 \cdot \text{OEt}_2$ , a typically non-chelating Lewis acid.<sup>8,9</sup> Dipole minimization of the O–B bond of the monocoordinated Lewis acid/substrate complex and the O–C  $\beta$ -alkoxy group were the proposed origin of the observed selectivity (Figure 2, B).

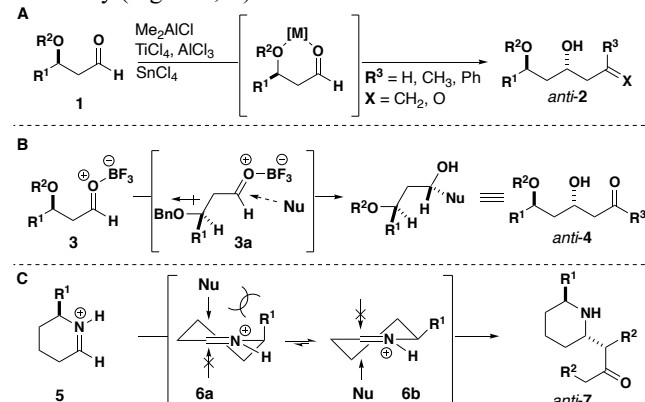


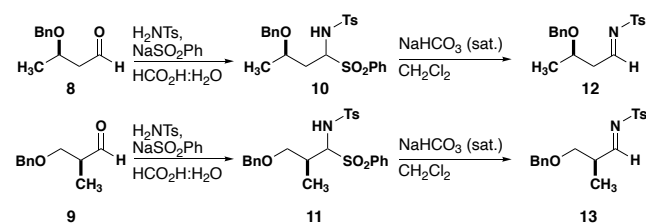
**Figure 2.** Lewis acid-mediated additions to  $\beta$ -alkoxy aldehydes.

While six-membered chelates have been reported to form and lead to *anti*-products in additions to  $\beta$ -alkoxy aldehydes, conformational preferences of the chelate are not typically discussed. In a conformationally related reaction, Stevens uses stereoelectronic arguments to rationalize the highly selective reactions of vinyl alcohols and tetrahydropyridinium ions that adopt half-chair conformers resembling **6a** and **6b** (Figure 2, C).<sup>10</sup> *Anti*-7 ultimately arises from nucleophilic attack on conformer **6b** from a mode of attack that avoids formation of twist-boat products or build up of 1,3 diaxial strain. Taking this model into consideration, should a six-membered chelate form in Lewis acid mediated additions to  $\beta$ -alkoxy *N*-Ts imines, stereoelectronic arguments similar to Stevens' rationale and Fürst-Plattner rules may be applied to predict and control for stereochemical outcomes of half-chair six-membered chelates.

Our investigation of  $\beta$ -alkoxy *N*-Ts imines utilizes 1,3 asymmetric induction to access *anti*-1,3 amino alcohols. Furthermore, the observed diastereomeric ratios provide insight into: (1) the influence of the conformational preferences of the six-membered ring chelate (2) the origin of selectivity when  $\text{BF}_3 \cdot \text{OEt}_2$ , a non-chelateable Lewis acid, is employed. The results of our investigation can help to construct a generalized model that describes the diastereomeric outcomes of additions to  $\beta$ -alkoxy carbon electrophiles.

We began our studies with allylations to imines **12** and **13** for a direct comparison to the allylations performed previously on the analogous aldehydes. Synthetic access to imines **12** and **13** was achieved in a couple of steps from the known analogous aldehyde precursors **8** and **9**, through precipitation and isolation of amidosulfones **10** and **11** (Scheme 1). We hypothesized that should a six-membered chelate form, the *anti* product would predominate, such as in the case of the analogous aldehydes.

### Scheme 1. Synthesis of Imines 12 and 13



*Anti*-14 was the major product in allylations of imine **12** with allyltrimethylsilane regardless of Lewis acid employed (Table 1).  $\text{AlCl}_3$ ,  $\text{SnCl}_4$  and  $\text{Cu}(\text{OTf})_2$  provided the best yields and

Table 1. Lewis Acid-Mediated Allylations to Imine 12

Entry	[M]	Lewis-acid	Solvent	Temp (°C)	<i>anti</i> : <i>syn</i> <sup>a</sup>	yield <sup>b</sup>
1	TMS	$\text{ZnBr}_2$	$\text{CH}_2\text{Cl}_2$	-78 to rt	73:27	90%
2	TMS	$\text{ZnI}_2$	$\text{CH}_2\text{Cl}_2$	-78 to rt	78:22	32%
3	TMS	$\text{AlCl}_3$	$\text{CH}_2\text{Cl}_2$	-78 to rt	81:19	96%
4	TMS	$\text{SnCl}_4$	$\text{CH}_2\text{Cl}_2$	-78 to rt	80:20	92%
5	TMS	$\text{TiCl}_4$	$\text{CH}_2\text{Cl}_2$	-78 to rt	78:22	41%
6	TMS	$\text{TiOH}$	$\text{CH}_2\text{Cl}_2$	-78 to rt	82:18	57%
7	TMS	$\text{BF}_3 \cdot \text{OEt}_2$	$\text{CH}_2\text{Cl}_2$	-78 to rt	81:19	49%
8	TMS	$\text{BF}_3 \cdot \text{OEt}_2$	$\text{CHCl}_3$	-20	81:19	26%
9	TMS	$\text{Cu}(\text{OTf})_2$	$\text{CH}_2\text{Cl}_2$	-78 to rt	79:21	72%
10	TMS	$\text{Cu}(\text{OTf})_2$	$\text{PhMe}$	-78 to -20	80:20	94%
11	$\text{BF}_3 \cdot \text{K}$	$\text{BF}_3 \cdot \text{OEt}_2$	$\text{CHCl}_3$	-20	68:32	13%
12	Bpin	$\text{BF}_3 \cdot \text{OEt}_2$	$\text{CH}_2\text{Cl}_2$	-78 to rt	n.d.	n.d.
13	$\text{SnBu}_3$	$\text{AlCl}_3$	$\text{CH}_2\text{Cl}_2$	-78 to rt	76:24	60%
14 <sup>c</sup>	TMS	$\text{Cu}(\text{OTf})_2$	$\text{CH}_2\text{Cl}_2$	-78 to rt	n.d.	n.d.

<sup>a</sup>*anti*:*syn* ratios determined by integration of  $^1\text{H}$  NMR spectra of unpurified reaction mixtures.

<sup>b</sup>Yields obtained by integration of  $^1\text{H}$  NMR spectra with 1,3,5-trimethylbenzene as the internal standard.

<sup>c</sup>Reaction run with 2.0 equiv. of 2,6-di-*tert*-butylpyridine.

diastereomeric ratios of product for the reaction (Table 1, entries 3, 4 and 9). The *anti* selectivity observed for most Lewis acids can be rationalized through stereoelectronic considerations of each mode of attack on half-chair conformers **15a** and **15b** (Figure 3). Ruling out the trajectories of attack that lead to twist-boat products, approach of the nucleophile to the six-membered ring chelate is sterically unhindered in the case of lower energy half-chair conformer **15a** while sterically hindered on the higher energy conformer **15b**. Stereoelectronic interactions of nucleophilic attack and conformational preferences of the chelate are reinforcing in this case and predict for the major *anti*-13 product observed.

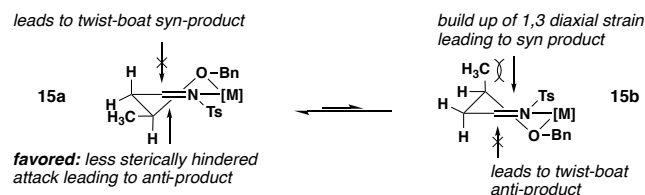


Figure 3. Four modes of nucleophilic attack on conformers **15a** and **15b**.

The typically non-chelatable Lewis acid  $\text{BF}_3 \cdot \text{OEt}_2$  also resulted in *anti* selectivity (Table 1, entries 3 and 7). The major *anti* product observed with  $\text{BF}_3 \cdot \text{OEt}_2$  suggests that the dipolar mechanism proposed previously by Evans does not adequately explain the analogous reaction with *N*-Ts imine (Figure 4). Where  $\text{BF}_3$  would preferentially bind Z to the H substituent on the C=O bond of **3** (Figure 2),  $\text{BF}_3$  is forced to bind Z to the alkyl substituent of imine **12** due to the presence of the *N*-tosyl group. To achieve the minimization of dipoles in the analogous aldehyde substrate, one would have to rotate the C–O bond of the  $\beta$ -alkoxy bond 180 °C from its orientation in **3a** (Figure 2). This would result in nucleophilic attack that avoids steric interactions with the  $\beta$ -methyl substituent, leading to *syn*-14 instead of the *anti*-14 product observed. (Figure 4).

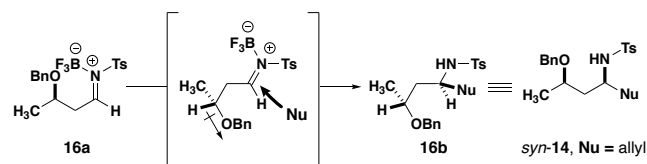


Figure 4. Consideration of dipolar effects previously proposed on  $\text{BF}_3 \cdot \text{OEt}_2$  mediated additions to imine **11**.

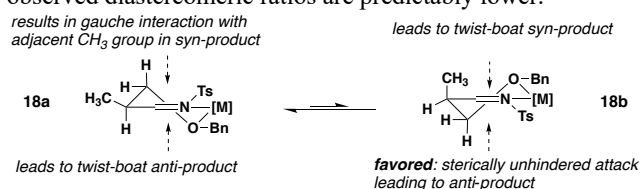
Imine **13** was synthesized to further probe the conformational preferences of the presumed six-membered ring chelate. If steric crowding of one face of the chelate governed selectivity alone without any conformational considerations of the

Table 2. Lewis Acid-Mediated Allylations to Imine 12

Entry	[M]	Lewis-acid	Solvent	Temp (°C)	<i>anti</i> : <i>syn</i> <sup>a</sup>	yield <sup>b</sup>
1	TMS	$\text{ZnBr}_2$	$\text{CH}_2\text{Cl}_2$	-78 to rt	68:32	80%
2	TMS	$\text{ZnI}_2$	$\text{CH}_2\text{Cl}_2$	-78 to rt	29:71	6%
3	TMS	$\text{AlCl}_3$	$\text{CH}_2\text{Cl}_2$	-78 to rt	82:18	93%
4	TMS	$\text{SnCl}_4$	$\text{CH}_2\text{Cl}_2$	-78 to rt	71:29	32%
5	TMS	$\text{TiCl}_4$	$\text{CH}_2\text{Cl}_2$	-78 to rt	75:25	73%
6	TMS	$\text{TiOH}$	$\text{CH}_2\text{Cl}_2$	-78 to rt	50:50	52%
7	TMS	$\text{FeCl}_3$	$\text{CH}_2\text{Cl}_2$	-78 to rt	56:44	95%
8	TMS	$\text{Cu}(\text{OTf})_2$	$\text{CH}_2\text{Cl}_2$	-20	60:40	88%
9	TMS	$\text{BF}_3 \cdot \text{OEt}_2$	$\text{CHCl}_3$	-20	50:50	92%
10	$\text{BF}_3 \cdot \text{K}$	$\text{BF}_3 \cdot \text{OEt}_2$	$\text{CHCl}_3$	-20	52:48	53%

<sup>a</sup>*anti*:*syn* diastereomeric ratios determined by integration of  $^1\text{H}$  NMR spectra of unpurified reaction mixtures. <sup>b</sup>Yields obtained by integration of  $^1\text{H}$  NMR spectra with 1,3,5-trimethylbenzene as the internal standard.

electrophile, a marked improvement in selectivity should be observed in imine **13** when compared to imine **12**. *Anti*-**17** was formed in comparable selectivity only when AlCl<sub>3</sub> was used as the Lewis acid (Table 2, entry 3). With all other Lewis acids, diastereomeric ratios of nucleophilic additions to imine **13** were, on average, lower than what was observed in allylations to imine **12** (Table 1). Reactions using TfOH, Cu(OTf)<sub>2</sub> and BF<sub>3</sub>•OEt<sub>2</sub> were all unselective (Table 2, entries 6, 8 and 9). The half-chair-like conformation invoked previously for imine **12** rationalizes the observed lower diastereomeric ratios for imine **13**. Fürst-Plattner approach (avoidance of twist-boat products) of the nucleophile on lower energy conformer **18a** is sterically unfavored as its trajectory is hindered by approach gauche to the methyl substituent (Figure 5). On the other hand, Fürst-Plattner approach is sterically unincumbered in conformer **18b**, though **18b** is presumed to be higher in energy relative to that of conformer **17a** due to bearing a pseudoaxial methyl group. As Fürst-Plattner rules are not reinforcing with the favored half-chair conformer of the chelate resulting from imine **13**, the observed diastereomeric ratios are predictably lower.



**Figure 5.** Consideration of Fürst-Plattner rules for additions to **18a** and **18b**.

To explore a wider range of substrates, multicomponent reaction (MCR) conditions previously used to generate *N*-Cbz imines from chiral aldehydes *in situ* were optimized for reactions using *N*-Ts imines (Table 3).<sup>11, 12</sup> These conditions avoid the requisite precipitation of the amido-sulfone intermediates, which is strongly substrate-dependent and does not consistently produce a solid, preventing isolation. Observed diastereomeric ratios using MCR conditions and Cu(OTf)<sub>2</sub> matched with the diastereomeric ratios using amidosulfone derived imines and the same Lewis acid (Table 3, entry 6). Unlike the other Lewis acids used under MCR conditions, Cu(OTf)<sub>2</sub> preferentially mediated addition to the imine rather than the aldehyde and resulted in no detectable aldehyde addition product. However, reactions using Cu(OTf)<sub>2</sub> led to no observed product in the presence of proton scavenger 2,6-di-*tert*-butylpyridine (Table 3, entry 12). This observation accompanied by the analogous experiment performed on

**Table 3. Lewis Acid-Mediated Allylations of Aldehyde 7 Using MCR Conditions**

Entry	Lewis-acid	Solvent	Temp (°C)	<i>anti</i> : <i>syn</i> <sup>a</sup>	% addition to <b>8</b> <sup>a</sup>
1	BF <sub>3</sub> •OEt <sub>2</sub>	MeCN	0	60:40	5
2	BF <sub>3</sub> •OEt <sub>2</sub>	CH <sub>2</sub> Cl <sub>2</sub>	-20	79:21	35
3	AlCl <sub>3</sub>	CH <sub>2</sub> Cl <sub>2</sub>	-20	68:32	19
4	SnCl <sub>4</sub>	CH <sub>2</sub> Cl <sub>2</sub>	-20	68:32	11
5	TiCl <sub>4</sub>	CH <sub>2</sub> Cl <sub>2</sub>	-20	70:30	24
6	Cu(OTf) <sub>2</sub>	CH <sub>2</sub> Cl <sub>2</sub>	-20	82:18	—
7	Cu(OTf) <sub>2</sub>	MeCN	-20	60:40	—
8	Cu(OTf) <sub>2</sub>	PhMe	-20	80:20	—
9	Cu(OTf) <sub>2</sub>	CH <sub>2</sub> Cl <sub>2</sub>	-20	80:20	—
10	Cu(OTf) <sub>2</sub>	CH <sub>2</sub> Cl <sub>2</sub>	0	82:18	—
11	Cu(OTf) <sub>2</sub>	CH <sub>2</sub> Cl <sub>2</sub>	rt	80:20	—
12 <sup>b</sup>	Cu(OTf) <sub>2</sub>	CH <sub>2</sub> Cl <sub>2</sub>	rt	n.d.	n.d.
13	TfOH	CH <sub>2</sub> Cl <sub>2</sub>	-20	75:25	4

<sup>a</sup>Determined by integration of <sup>1</sup>H NMR spectra of unpurified reaction mixtures. <sup>b</sup>Reaction run with 2.0 equiv. of 2,6-di-*tert*-butylpyridine.

isolated imine **12** (see Table 1, entry 14) led to the conclusion that the reaction with Cu(OTf)<sub>2</sub> likely proceeds through formation of an iminium ion and observed diastereomeric ratios result from intramolecular hydrogen bonding, or proton-chelation. Previous reports also corroborate proton-chelation in the case of *N*-Cbz and *N*-Ts imines.<sup>1, 11</sup>

With optimized MCR conditions, aldehydes **20a–20h** were converted to allylated products **21a–21h** using MCR conditions **B** (Table 4). Diastereomeric ratios trended upwards with steric bulk at the R<sup>1</sup> position. Employment of *tert*-butyl-diphenylsilyl (TBDPS) group at R<sup>2</sup> resulted in complete erosion of selectivity for the reaction (Table 4, entry 1). Sterically hindered silyl ether substituents have less binding affinity for Lewis acids, disfavoring chelate formation.<sup>6</sup> Aldehyde **19g** produced an equal mixture of diastereomeric products, presumably due to bearing methyl substituents on both sides of the preformed chelate (Table 4, entry 7). Allylation of **19h** resulted in major diastereomer *anti*-**20h** in 67:33 ratio (Table 4, entry 8), despite compounded steric bulk to one side of the chelate.

**Table 4. MCR Scope**

Entry	19/20	R <sup>1</sup>	R <sup>2</sup>	R <sup>3</sup>	R <sup>4</sup>	Conditions A <i>anti</i> : <i>syn</i> <sup>a</sup> (yield%)	Conditions B <i>syn</i> : <i>anti</i> <sup>a</sup> (yield%)
1	a	CH <sub>3</sub>	TBDPS	H	H	—	54:46 (70)
2	b	CH <sub>3</sub>	Bn	H	H	79:21 (72)	78:22 (44)
3	c	<i>n</i> -Bu	Bn	H	H	83:17 (74)	78:22 (55)
4	d	<i>i</i> -Pr	Bn	H	H	89:11 (45)	81:19 (37)
5	e	<i>t</i> -Bu	Bn	H	H	—	89:11 (44)
6	f	Ph	Bn	H	H	95:5	92:8 (76)
7	g	CH <sub>3</sub>	Bn	CH <sub>3</sub>	H	—	49:51 (60)
8	h	CH <sub>3</sub>	Bn	H	CH <sub>3</sub>	—	67:33 (47 <sup>e</sup> )

<sup>a</sup>*anti*:*syn* ratios determined by integration of <sup>1</sup>H NMR spectra of unpurified reaction mixtures.

<sup>b</sup>Yield obtained by integration of <sup>1</sup>H NMR spectra with 1,3,5-trimethylbenzene as the internal standard.

Computational studies were conducted using Gaussian16<sup>13</sup> to rationalize the diastereomeric ratios of products resulting from allylations to **20**. The B3LYP<sup>14</sup> density functional with the 6-31G(d,p) basis set was selected for geometry optimizations and free energy calculations for each conformer due to its demonstrated applicability to systems analogous to it.<sup>1</sup> Calculations reveal that formation of the proton-chelate **22** is energetically favorable and that the chelate can adopt two half-chair-like conformations **23b** and **24b** (Figure 6). Assuming that the facial trajectory of nucleophilic attack is best described by Fürst-Plattner rules with the formation of twist-boat products energetically unlikely, the magnitude of diastereoselectivity observed is best represented by the overall energy difference between conformers **23b** and **24b** of the proton chelate.

To test this hypothesis, the relative energy differences between the two half-chairs possible of chelates **23** and **24** were

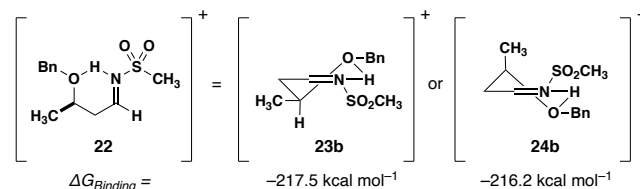
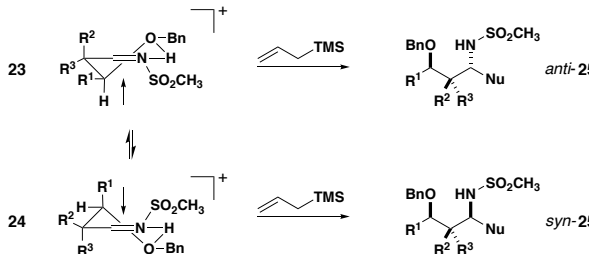


**Figure 6.** Calculated  $\Delta G_{\text{binding}} = \Delta G(22) - (\Delta G(12) + \Delta G(H^+))$  for proton-chelate **22**.

calculated using the same functional and basis set (Table 6). Differences in free energies of **23** and **24** were then correlated to observed diastereomeric ratios of products (Figure 7). All observed diastereomeric ratios correlated well with the magnitude of computed  $\Delta G(\mathbf{23}:\mathbf{24})$  with the exception of *tert*-butyl (Table 6, entries 4). Conformer **24e** bearing pseudoaxial  $R^1=t$ -Bu was the computed lowest energy chelate-conformer for the *tert*-butyl substituted chelate. However, on this conformer, Fürst-Plattner attack would result in the build-up of significant 1,3 diaxial strain analogous to the one depicted in conformer **15b** (Figure 3). So, while **24e** is a competitive conformer to **23e**, **23e** is more reactive and leads to the *anti* product. This would be consistent with transition state energies reflecting the ultimate product ratios described by Curtin-Hammett principles for bulkier substituents like *tert*butyl. On the other hand, diastereomeric ratios observed with smaller substituents on the chelate depend more closely on the energy differences between their chelate conformers.

**Table 6. Computed Free Energy Differences of **23** and **24****



Entry	R <sup>1</sup>	R <sup>2</sup>	R <sup>3</sup>	% of <i>anti</i> - <b>21</b>	Computed $\Delta G$ of <b>23:24</b>	% Major Conformer
1	CH <sub>3</sub>	H	H	<b>21b</b> , 80	1.36	91
2	<i>n</i> -Bu	H	H	<b>21c</b> , 78	1.00	85
3	<i>i</i> -Pr	H	H	<b>21d</b> , 81	0.80	80
4	<i>t</i> -Bu	H	H	<b>21e</b> , 89	0.54	71
5	Ph	H	H	<b>21f</b> , 92	2.23	98
6	CH <sub>3</sub>	H	CH <sub>3</sub>	<b>21g</b> , 50	0.01	51
7	CH <sub>3</sub>	CH <sub>3</sub>	H	<b>21h</b> , 67	0.73	77

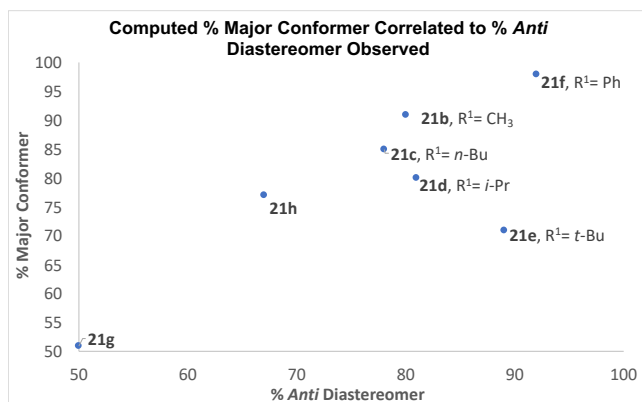


**Figure 7.** Graphical representation of correlation between computed % major conformer (**23** or **24**) and % *anti*-**21** observed

To conclude, we have developed two optimized allylation reaction conditions for access to *anti*-1,3 amino alcohols either from  $\beta$ -alkoxy imine or aldehyde starting materials. Experimental and computational results show that Cu(OTf)<sub>2</sub> mediated allylations of  $\beta$ -alkoxy imines are preceded by formation of a proton-chelate that can adopt two half-chair-like conformations. The observed diastereoselectivity of addition to the chelate is influenced by stereoelectronic interactions

between half-chair chelates and nucleophile, as well as the conformational preferences of the chelate itself. The stereoelectronic considerations described herein resemble that of Fürst-Plattner rules and have been previously proposed to rationalize stereochemical outcomes of addition to tetrahydropyridinium ions. Together, we have proposed a generalizable stereoelectronic model describing nucleophilic additions to  $\beta$ -alkoxy imines, which will inform retrosynthetic planning of stereochemically-complex nitrogen-containing targets.

## ASSOCIATED CONTENT

### Supporting Information

Supporting information (experimental procedures, X-ray crystallographic data, <sup>1</sup>H and <sup>13</sup>C NMR spectra, and computational details) is available free of charge.

## AUTHOR INFORMATION

### Corresponding Author

\*E-mail: jtshaw@ucdavis.edu

## ACKNOWLEDGMENT

Research reported in this publication was supported by the National Science Foundation ( grant codes here ). J.S.F. acknowledges the computational resources provided by UCLA Institute for Digital Research and Education and the National Science Foundation through XSEDE Science Gateways Program (TG-CHE040013N). We thank Prof. Dean Tantillo for providing guidance on the computational work reported herein. We thank the National Science Foundation (Grant CHE-1531193) for the dual source X-ray diffractometer.

## REFERENCES

- (1) Moore, L. C.; Lo, A.; Fell, J. S.; Duong, M. R.; Moreno, J. A.; Rich, B. E.; Bravo, M.; Fetting, J. C.; Souza, L. W.; Olmstead, M. M.; Houk, K. N.; Shaw, J. T., *Chem. Eur. J. Soc.* **2019**, 25 (52), 12214-12220.
- (2) Lait, S. M.; Rankic, D. A.; Keay, B. A., *Chem. Rev.* **2007**, 107 (3), 767-796.
- (3) Palchykov, V. A.; Gaponov, A. A., Chapter Four - 1,3-Amino alcohols and their phenol analogs in heterocyclization reactions. In *Adv. Heterocycl. Chem.*, Scriven, E. F. V.; Ramsden, C. A., Eds. Academic Press: 2020; Vol. 131, pp 285-350.
- (4) Reetz, M. T.; Jung, A., *J. Am. Chem. Soc.* **1983**, 105 (14), 4833-4835.
- (5) Keck, G. E.; Castellino, S., *J. Am. Chem. Soc.* **1986**, 108 (13), 3847-3849.
- (6) Keck, G. E.; Castellino, S.; Wiley, M. R., *J. Org. Chem.* **1986**, 51 (26), 5478-5480.
- (7) Kiyooka, S.-i.; Heathcock, C. H., *Tetrahedron Lett.* **1983**, 24 (44), 4765-4768.
- (8) Evans, D. A.; Duffy, J. L.; Dart, M. J., *Tetrahedron Lett.* **1994**, 35 (46), 8537-8540.
- (9) Evans, D. A.; Dart, M. J.; Duffy, J. L.; Yang, M. G., *J. Am. Chem. Soc.* **1996**, 118 (18), 4322-4343.
- (10) Evans, D. A.; Allison, B. D.; Yang, M. G.; Masse, C. E., *J. Am. Chem. Soc.* **2001**, 123 (44), 10840-10852.
- (11) Ella-Menye, J.-R.; Dobbs, W.; Billet, M.; Klotz, P.; Mann, A., *Tetrahedron Lett.* **2005**, 46 (11), 1897-1900.
- (12) Pasunooti, K. K.; Leow, M. L.; Vedachalam, S.; Gorityala, B. K.; Liu, X.-W., *Tetrahedron Lett.* **2009**, 50 (24), 2979-2981.
- (13) Frisch, M. J.; Trucks, G. W.; Schlegel, H. B.; Scuseria, G. E.; Robb, M. A.; Cheeseman, J. R.; Scalmani, G.; Barone, V.; Petersson, G. A.; Nakatsuji, H.; Li, X.; Caricato, M.; Marenich, A. V.; Bloino, J.; Janesko, B. G.; Gomperts, R.; Mennucci, B.; Hratchian, H. P.;

Ortiz, J. V.; Izmaylov, A. F.; Sonnenberg, J. L.; Williams; Ding, F.; Lipparini, F.; Egidi, F.; Goings, J.; Peng, B.; Petrone, A.; Henderson, T.; Ranasinghe, D.; Zakrzewski, V. G.; Gao, J.; Rega, N.; Zheng, G.; Liang, W.; Hada, M.; Ehara, M.; Toyota, K.; Fukuda, R.; Hasegawa, J.; Ishida, M.; Nakajima, T.; Honda, Y.; Kitao, O.; Nakai, H.; Vreven, T.; Throssell, K.; Montgomery Jr., J. A.; Peralta, J. E.; Ogliaro, F.; Bearpark, M. J.; Heyd, J. J.; Brothers, E. N.; Kudin, K. N.; Staroverov, V. N.; Keith, T. A.; Kobayashi, R.; Normand, J.; Raghavachari, K.; Rendell, A. P.; Burant, J. C.; Iyengar, S. S.; Tomasi, J.; Cossi, M.; Millam, J. M.; Klene, M.; Adamo, C.; Cammi, R.; Ochterski, J. W.; Martin, R. L.; Morokuma, K.; Farkas, O.; Foresman, J. B.; Fox, D. J. *Gaussian 16 Rev. C.01*, Wallingford, CT, 2016.

(14) Becke, A. D., *J. Chem. Phys.* **1993**, 98 (7), 5648-5652.

---